Published in final edited form as:
J Mol Biol. 2008 June 13; 379(4): 704–718. doi:10.1016/j.jmb.2008.04.026.

Effect of lipid composition on the topography of membrane-associated hydrophobic helices:

stabilization of transmembrane topography by anionic lipids

Khurshida Shahidullah and **Erwin London**
Dept. of Biochemistry and Cell Biology, Stony Brook University, Stony Brook, NY 11794-5215

Abstract

To investigate the effect of lipid structure upon the membrane topography of hydrophobic helices, the behavior of hydrophobic peptides was studied in model membrane vesicles. To define topography, fluorescence and fluorescence quenching methods were used to determine the location of a Trp at the center of the hydrophobic sequence. For peptides with cationic residues flanking the hydrophobic sequence, the stability of the transmembrane (TM) configuration (relative to a *membrane-bound* non-TM state) increased as a function of lipid composition in the order: 1:1 (mol:mol) 1-palmitoyl-2-oleoyl phosphatidylcholine (POPC):1-palmitoyl-2-oleoyl phosphatidylethanolamine (POPE) ~ 6:4 POPC:cholesterol < POPC ~ dioleoylphosphatidylcholine (DOPC) < dioleoylphosphatidylglycerol (DOPG) ≤ dioleoylphosphatidylserine (DOPS), indicating that the anionic lipids DOPG and DOPS most strongly stabilized the TM configuration. TM-stabilization was near-maximal at 20-30mol% anionic lipid, physiologically relevant values. TM-stabilization by anionic lipid was observed for hydrophobic sequences with diverse set of sequences (including polyAla), diverse lengths (from 12-22 residues), and various cationic flanking residues (H, R or K), but not when the flanking residues were uncharged. TM-stabilization by anionic lipid was also dependent on the number of cationic residues flanking the hydrophobic sequence, but was still significant with only one cationic residue flanking each end of the peptide. These observations are consistent with TM-stabilizing effects being electrostatic in origin. However, Trp located more deeply in DOPS vesicles relative to DOPG vesicles, and peptides in DOPS vesicles showed increased helix formation relative to DOPG and all other lipid compositions. These observations fit a model in which DOPS anchors flanking residues near the membrane surface more strongly than does DOPG, and/or increases the stability of the TM state to a greater degree than DOPG. We conclude anionic lipids can have significant and headgroup structure-specific effects upon membrane protein topography.

Keywords

Membrane proteins; fluorescence; fluorescence quenching; phosphatidylserine; phosphatidylglycerol

INTRODUCTION

The fact that interior of the bilayer is hydrophobic leads to the expectation that helical TM sequences should be composed of hydrophobic amino acids. On the other hand, TM sequences can contain a significant number of hydrophilic residues if required by helix-helix interactions

Corresponding author info: Erwin London Dept. of Biochemistry and Cell Biology Phone: 631-632-8564 Fax: 631-632-8575 Email: Erwin.London@stonybrook.edu.

or specific functions, as is evident for membrane pumps and ion channels in which numerous charged and polar residues are tolerated within generally non-polar TM segments[1,2].

Nevertheless, too many hydrophilic residues in the hydrophobic core can lead to a less stable TM topography resulting in the formation of a non-TM state in aqueous solution or membrane-bound but located close to the membrane surface[3-5]. The equilibrium between TM and non-TM topographies can be functionally significant. Bacterial protein toxins form the most widely studied examples of proteins with this behavior. The hydrophobic helices of diphtheria toxin T domain undergo TM/non-TM interconversion thought to be essential for translocation across membranes[6,7]. This interconversion also occurs in the membrane-inserting segments of beta-barrel toxins, including anthrax toxin protective antigen[8] and cholesterol-dependent cytolysins[9,10]. It is also believed to be important for some Bcl family proteins (involved in apoptosis)[11], a number of tail-anchored endoplasmic reticulum enzymes,[12] polio virus 3A protein[13], and antimicrobial peptides[14].

TM topography can be regulated by lipid composition. For example, it has been reported that bacterial lipid composition affects the topography of TM helices in complex membrane proteins[15,16]. Certain bacterial cytolysins require cholesterol to form a TM state[17], and the T domain of diphtheria toxin forms a TM state more easily in bilayers composed of lipids with short acyl chains[7]. The question of modulation of TM protein topography and function by lipid composition is also interesting in eukaryotic membranes because the lipid environment of many membrane proteins varies as they cycle between various internal membranes and the plasma membrane. Nevertheless, little is known mechanistically about what effect the structural diversity of membrane lipids has in controlling TM topography.

In this report, we studied the effect of lipid composition on hydrophobic helix behavior using synthetic peptides incorporated into model membrane vesicles (“liposomes”). Synthetic hydrophobic peptides, frequently Lys-flanked polyLeu or polyLeu-Ala helices, have been successfully utilized as models for hydrophobic α-helical TM domains by our lab and many others[18-24]. In this report fluorescence spectroscopy was used to study the lipid composition-dependence of the TM stability of these and closely related sequences. We found that physiological membrane concentrations of anionic lipids greatly stabilize the TM conformation of the hydrophobic helices flanked by cationic residues. In addition, there was a marked difference between topography in the presence of two different anionic lipids. This was true for peptide sequences with diverse hydrophobic sequences, short or long hydrophobic lengths, and various cationic flanking residues. It is likely that these properties are important for the function of these lipids.

RESULTS

Distinguishing TM and non-TM Topographies

The effect of lipid composition upon the topography of a variety of bilayer-inserted hydrophobic sequences was studied. The peptides had hydrophobic cores with a variety of lengths and hydrophobicities, and their hydrophobic sequences were flanked by ionizable hydrophilic residues (Table 1). The peptides also contained a Trp in the center of the hydrophobic sequence. Measurement of Trp location within the membrane allows identification of membrane topography[3,5,25,26]. Since Trp emission is sensitive to the polarity of its surrounding environment, one method to measure Trp location is from its fluorescence emission λmax. For the peptides in this study, in a fully TM orientation a Trp residue at the center of the sequence locates at the center of the highly non-polar core of the lipid bilayer and exhibits a highly blue-shifted λmax near 320-325 nm[27,28]. When a peptide adopts a membrane-bound non-TM orientation, its hydrophobic core moves close to the more polar bilayer surface, and Trp λmax exhibits a strong red shift, falling in the range of

335-345nm[27,28]. Intermediate values of Trp λmax can be indicative of mixed populations of TM and non-TM topographies, but can also be observed when a conformation forms in which Trp is at an intermediate depth[28,29].

To confirm TM topography using a more direct method, dual fluorescence quenching was also used to measure Trp depth. In this method, Trp fluorescence quenching is compared using two molecules: 10-doxylnonadecane (10-DN), a bilayer inserted quencher that quenches Trp deeply buried within the membrane strongly, and acrylamide, a water soluble quencher that quenches Trp most strongly when the Trp is exposed to aqueous solution. The ratio of acrylamide quenching to 10-DN quenching (quenching ratio or Q-ratio) exhibits a linear relationship with Trp depth[29]. A low quenching ratio of <0.1-0.2 is indicative of a Trp located near the bilayer center and a high Q-ratio ≥1 is observed for a Trp located close to the bilayer surface. Intermediate Q-ratios can be observed for mixed populations of deep and shallow Trp, or when a conformation forms in which Trp is at an intermediate depth[28,29].

A third method to define the topography of hydrophobic helices is to measure how Trp fluorescence is affected by bilayer width. Hydrophobic helices that can form a TM configuration are sensitive to hydrophobic mismatch, which is the difference between the length of a hydrophobic helix and the width of the hydrophobic core of the bilayer. Such sequences exhibit Trp emission that is sensitive to bilayer width. Trp emission red shifts in wide bilayers due to negative mismatch-induced destabilization of the TM state, and formation of a significant amount of a non-TM state[3,25]. Emission also red shifts in very thin bilayers, partly due to positive mismatch[26]. The result is a "U" shaped dependence of λmax upon bilayer width. In contrast, when a hydrophobic helix is bound to membrane in a non-TM location close to the bilayer surface it emits red-shifted fluorescence with a λmax that is insensitive to bilayer width[3].

The Stability of the TM Topography of Hydrophobic Helices with Varying Hydrophobicities: Effect of Bilayer Width

First, the membrane topography of a series of peptides containing Leu/Ala-rich hydrophobic cores was measured. Hydrophobicity was varied by varying the content of Leu and Ala residues from 15 Leu 0 Ala (most hydrophobic, $^{KK}pL_{15}(D10)$) to 7 Leu 8 Ala (most hydrophilic, $^{KK}pL_7A_8(D10)$) (Table 1, sequences 1-5). To allow evaluation of peptide topography the peptides also contained a single Trp at the center of the hydrophobic sequences. An Asp was also present at the center of the hydrophobic sequence so that the hydrophobicity of the peptides could be controlled with pH.

Trp emission λmax was measured as a function of bilayer width by incorporating the peptides into vesicles composed of phosphatidylcholines containing monounsaturated acyl chains of various lengths (Figure 1). Under low pH conditions (+), in which the Asp residue should be uncharged (see below), most of the peptides exhibited a U-shaped dependence of λmax on bilayer width with a minimum λmax ~320-325 nm, indicative of a TM topography in bilayers with an intermediate width (e.g. with 18:1 acyl chains). The exception was the most hydrophilic peptide tested ($^{KK}pL_7A_8(D10)$) which showed a red shifted λmax (335-340 nm) that was not very dependent on bilayer width. This indicates that $^{KK}pL_7A_8(D10)$ does not form a TM state in these vesicles at low pH. (Instead, the peptide is bound to the bilayer surface, see below.)

Under high pH conditions (Δ), in which the Asp residue should be charged (see below), all of the peptides exhibited red shifted fluorescence that was not very dependent on bilayer width. This indicates that when the Asp residue is charged the peptides are not hydrophobic enough to form a TM topography. The Trp λmax values observed in most cases (335-345 nm) were indicative of peptides bound to the bilayer surface. The $^{KK}pL_7A_8(D10)$ peptide exhibited even

more highly red-shifted fluorescence (λmax ~350 nm, off scale in Figure 1) indicative of peptide that is dissolved, or at least largely dissolved, in aqueous solution.

Most subsequent experiments were carried out at pH 4 so that the Asp residue would be uncharged. However, when DOPS vesicles were used, pH was generally kept at 5.5 so that the PS carboxyl group would not be protonated, and PS would retain a net negative charge[30,31]. This was not necessary for PG which ionizes at a somewhat lower pH than PS[32].

Effect of Lipid Structure Upon the Stability of The TM Topography of Hydrophobic Helices With Varying Hydrophobicities: Vesicles with No Net Charge

Next, the Trp fluorescence of these peptides was measured in a variety of lipids and lipid mixtures with different polar headgroups. Phospholipids containing 16 or 18 carbon atom long acyl chains, which are common in biological membranes, were used. The phospholipids used had a least one 9-10 cis double bond in one of their acyl chains so that the lipid bilayers would be in the normal liquid disordered state[33].

Figure 2 shows Trp emission λmax (Figure 2A) and Q-ratios (Figure 2B, raw quenching data is in Supplemental Table S1) for these peptides when incorporated into lipid vesicles with various compositions lacking a net electric charge (DOPC, POPC, 1:1 POPC/POPE mol:mol, and 6:4 mol:mol POPC/cholesterol). In all cases, the most hydrophobic peptide ($^{KK}pL_{15}(D10)$) exhibited a blue-shifted λmax and low Q-ratio value typical for TM helices with a Trp at the center of the bilayer, while the red shifted λmax and high Q-ratio values were observed for the least hydrophobic peptide ($^{KK}pL_7A_8(D10)$) corresponding to a fully non-TM state[3,34]. The peptides with intermediate numbers of Ala showed intermediate λmax and Q-ratio values that tended to increase as the number of Ala increased, consistent with progressively less stable TM orientation as the hydrophobicity of the peptides decreased. It should be noted that previous studies show similar effects of the Leu to Ala ratio upon the stability of the TM topography[4, 24].

For vesicles without net charge, the behavior of most of the peptides was only slightly dependent upon lipid structure (Figure 2). The main exception was the $^{KK}pL_7A_8(D10)$ peptide, which exhibited highest λmax (345-355nm) and Q-ratio values in POPC/POPE and POPC/cholesterol vesicles. These values indicate that a significant fraction of this peptide was either very shallowly located or not even membrane-bound in vesicles composed of these lipids.

The value of the pKa of the Asp residue also yields information concerning the location of these peptides. Because a charged Asp residue is energetically unfavorable in a hydrophobic environment[3,5,34], the pKa of an Asp residue in the center of a TM helix is much higher than in a state in which the Asp residue is located more shallowly in the membrane or fully exposed to aqueous solution, as in the case of a peptide located at the bilayer surface or dissolved in aqueous solution[5]. In fact, previous studies showed that the presence of a charged Asp buried within the lipid bilayer is so energetically unfavorable that ionization of an Asp in the middle of a TM helix is accompanied by conversion to the non-TM state[5], i.e. the TM/non-TM and Asp ionization equilibria are linked.

As shown inFigure 1 there were changes in Trp fluorescence due to ionization of the Asp residue, so that the Asp pKa values could be determined from wavelength shifts in the emission spectra as a function of pH (Supplemental Figure S1). Figure 3A gives apparent Asp pKa values for the peptides determined by this method as a function of the number of Ala residues when the lipids used have no net charge. Asp pKa decreased as the hydrophobicity of the peptide decreased (i.e. as the number of Ala increased). This suggest that when the Asp is protonated the stability of the TM state decreases as peptide hydrophobicity decreases, consistent with the λmax and quenching data. On the average, pKa values were slightly lower for vesicle

compositions containing POPE or cholesterol. This is consistent with a slightly lower stability of the TM state relative to a non-TM configuration in these lipids as compare to that in DOPC or POPC vesicles.

Effect of Lipid Structure Upon the Stability of The TM Topography of Hydrophobic Helices With Varying Hydrophobicities: Zwitterionic vs. Anionic Lipid Vesicles

In contrast to the results above, lipid charge had a large effect on the stability of the TM state. Generally, λmax was more blue shifted (Figure 4A) and the Q-ratio was lower (Figure 4B) when peptides were incorporated into vesicles composed of anionic lipids (DOPG or DOPS) than when incorporated into vesicles composed of zwitterionic and/or uncharged lipids. [This is most obvious for the least hydrophobic peptides, $^{KK}pL_9A_6(D10)$ and $^{KK}pL_7A_8(D10)$.] This behavior indicates that the TM state is significantly more stable in the vesicles composed of these anionic lipids.

It is noteworthy that Trp located more deeply in vesicles composed of DOPS than in vesicles composed of DOPG, with λmax and Q-ratio values in DOPS indicative of full formation of a TM state with the Trp at the bilayer center even in the case of the relatively hydrophilic $^{KK}pL_7A_8(D10)$ peptide. Additionally, pKa data indicated that the depth of the Asp group was deeper for peptides in DOPS vesicles than in DOPG vesicles (Figure 3B). The decrease in pKa as peptide hydrophobicity decreased was less in DOPS vesicles than in DOPG vesicles. Although the pKa of the Asp residues is much higher in anionic lipid vesicles than in vesicles lacking a net charge (compareFigure 3A and 3B) this may not be related to a difference in TM stability in anionic and zwitterionic vesicles. Instead, it reflects the well-known high proton concentrations close to the surface of anionic vesicles arising from the attraction of protons by the anionic charge on the lipid[31].

Importantly, the observation that Trp depth in DOPG vesicles was intermediate between the deep value observed in DOPS vesicles and the shallower values observed in vesicles lacking a net charge did not appear to involve the formation of a mixture of TM and non-TM topographies by peptides in DOPG vesicles but rather the formation of a single topography with an intermediate Trp and Asp depth. This reason for this statement is that we did not observe any large quencher-induced shifts in λmax. Such shifts are characteristic of co-existing populations with deep and shallow Trp depths because the relatively selective quenching of the deep population by 10-DN induces a large red shift of λmax while the quenching of the shallow population by acrylamide induces a large blue shift[29]. Instead of this, we observed only very small quencher-induced shifts (see Supplemental Table S2), behavior characteristic of cases in which there is an intermediate Trp depth[3,27]. This suggests that the difference between peptide behavior in the DOPG vesicles and DOPS vesicles arises from the way the TM state is anchored in the lipid bilayer (see Discussion).

It should also be noted that the differences between peptide behavior in DOPG and DOPS vesicles were not due to the difference in solution pH used in the λmax and Q-ratio experiments for these lipids. Control experiments showed that the λmax and Q-ratio values for peptides in DOPG vesicles was the same at pH 3.8 and 5.5, and that differential behavior of peptides in DOPG and DOPS vesicles could also be observed at neutral pH (Supplemental Table S3).

The Role of Cationic Flanking Residues in the Stabilization of the TM Conformation in Anionic Vesicles: Electrostatic Origin of Stabilization

The stabilization of the TM state observed for peptides inserted into anionic lipid vesicles could be due to electrostatic interactions between the charged residues and anionic lipids. To study this, we used a series of peptides lacking an Asp residue so that the charge of flanking residues could be varied without the complication of changes due to Asp ionization (Table 1, sequences

7-9). The peptides chosen had an inherently borderline TM stability due to their short hydrophobic segments[28]. To investigate the role of electrostatic effects, the effect of pH upon the stability of the TM state was compared in both zwitterionic and anionic vesicles when the peptides were flanked on both ends of the hydrophobic sequence by 2Lys ($^{KK}pL_{12}$), 2His ($^{HH}pL_{12}$), or 1Lys plus 1His residue ($^{KH}pL_{12}$).

Figure 5 illustrates the dependence of λmax and quenching upon flanking residue type and lipid composition at pH 5.5 and pH 9 for these peptides. Lys residues are charged at both of these pH values[5], while His residues should be largely protonated at pH 5.5 and largely deprotonated at pH 9. Consistent with this, in both anionic and zwitterionic vesiclesFigure 5 shows that there were pH-dependent changes in both Trp λmax and Q-ratio for a His-flanked peptide, but none for a peptide flanked only by Lys.

[In fact, for the $^{HH}pL_{12}$ peptide a change in fluorescence intensity upon pH titration detects one His pKa slightly above 5.5 and a pH-dependent shift in the Trp emission wavelength detects another pKa close to pH 7.5 for peptides incorporated into DOPC vesicles. In DOPS vesicles, the change in fluorescence intensity upon pH titration detects one His pKa near 6.5 and a pH-dependent shift in the Trp emission wavelength detects another close to pH ~8-8.3 (data not shown).]

Figure 5 also shows that at pH 5.5 Trp λmax blue shifted and Q-ratio were significantly lower in DOPS vesicles than in DOPC vesicles for all three peptides. This indicates that relative to topography in DOPC vesicles, in DOPS vesicles the TM state is stabilized relative to the non-TM state both when the flanking residues are charged Lys or charged His. This rules out stabilization of the TM state requiring a specific Lys-PS interaction. At pH 9, the λmax and Q-ratio data was similar to that at pH 5.5 for the Lys_2-flanked peptide, but for the His_2-flanked peptide there was no blue shift or decrease in Q-ratio in DOPS vesicles relative to that in DOPC vesicles. This indicates that when the His is not charged, DOPS does not stabilize the TM state, and thus the stabilization of the TM state is likely to be electrostatic in origin. In contrast, as noted above for the Lys-flanked peptide the λmax and Q-ratio data at pH 9 is similar to that at pH 5.5.

Figure 5 also shows that the behavior of the peptide with a hydrophobic core flanked by one His and one Lys exhibited intermediate behavior at high pH, with differences both in λmax and Q-ratio in DOPS vesicles relative to DOPC vesicles that were smaller than those for the peptide flanked by two Lys but larger than those for the peptide flanked by two His. This is expected as the peptide with one His and one Lys should carry a charge of +1 on each end at high pH, intermediate between that of the Lys_2(+2) and His_2(0) flanked peptides.

The Effect of Lipid Composition on the Stability of the TM State for Longer Helical Sequences

The studies above used peptides with relatively short, 12-17 residue hydrophobic cores. In these peptides the charged residues flanking the hydrophobic core would be somewhat more buried within the bilayer in the TM state than in the case of the longer ~20 residue hydrophobic sequences common in many TM proteins. The increased exposure of charged residues to a hydrophobic environment in the short peptides would tend to increase the free energy of the TM state for such sequences. Thus, it was possible that the stabilizing effects of anionic lipids upon peptide topography found above were specific to short hydrophobic helices.

To determine whether lipids have similar effects for longer hydrophobic sequences, peptides with hydrophobic cores of 18-22 residues long were studied. These sequences had weakly hydrophobic cores composed of Ala with or without a few Leu (Table 1, sequences 10-14). When these peptides were inserted into DOPS vesicles highly blue-shifted λmax and low Q-ratio values were generally observed (with the exception of $^{KK}pA_{22}$ peptide which showed a

somewhat more red shifted λmax and high Q-ratio), showing that a TM state predominated. In contrast, a non-TM state predominated in the presence of vesicles composed of DOPC (Table 2). This shows that stabilization of the TM state by DOPS is not restricted to short hydrophobic sequences. It should also be noted that stabilization of the TM configuration in DOPS vesicles relative to DOPC vesicles was similar for peptides with flanking Lys and Arg residues, indicating they interact similarly with DOPS.

Fluorescence properties indicated that in most cases the non-TM state formed in the presence of DOPC vesicles for these longer and less hydrophilic peptides was predominantly not vesicle-bound. First, Trp λmax, was close to that for free Trp and significantly more red shifted than for Trp located at the membrane surface[35]. Second, there was very little, if any, quenching of Trp fluorescence by the membrane-bound quencher 10-DN (Supplemental Table S1)[29].

An exception to this behavior was observed for the $^{KK}pL_4A_{18}$ peptide, which was slightly more hydrophobic than the other long peptides. It exhibited λmax and Q-ratio values indicating that the peptide was bound to the DOPC vesicles, similar to the behavior of the shorter hydrophobic sequences described above (Table 2). Also similar to the behavior of shorter hydrophobic sequences, the incorporation of cholesterol appeared to inhibit its binding to PC-containing vesicles, while λmax and Q-ratio values for this peptide incorporated into anionic lipids was lower than that in DOPC, with values in DOPG vesicles that were not as low as in DOPS vesicles. This shows that many of the effects of lipid structure upon topography described above are not restricted to shorter hydrophobic helices.

Behavior of Helical Peptides in Biologically Relevant Amounts of Anionic Lipids

The studies above used pure DOPS and DOPG vesicles. We were interested in whether anionic lipid effects would be similar in vesicles containing more physiologically relevant anionic lipid contents of 20-30mol%.Figure 6 shows that, as judged from Trp depth measured by Q-ratio, the stabilization of the TM state in vesicles composed of 30 mol%DOPS/70 mol% DOPC was almost as great as that in pure DOPS vesicles for a variety of peptides. [It should be noted that at the sample pH used peptide Asp residues were still protonated at lower anionic lipid contents, with a pKa value of ~ 6.5 at 30mol% DOPS (data not shown).]

Similarly, only a low mol% of DOPG was necessary to stabilize the TM state, with a significant degree of stabilization by as little as 5mol% DOPG (Figure 7). The mol% DOPG need to maximally stabilize the TM state (20 mol%) was similar for a peptide with four flanking Lys at each end of the hydrophobic sequence ($^{KKKK}pL_{11}A_4$(D10)) and a peptide with a less hydrophobic core, and only two flanking Lys at each end ($^{KK}pL_7A_8$(D10)), as judged by both Q-ratio (Figure 7A) and λmax (Figure 7B). It is noteworthy that for the latter peptide the increased stability of the TM state reached a plateau at 20mol% DOPG even though it has not formed a state with Trp as deep as in DOPS vesicles (see Discussion).

Secondary Structure Shows Increased Helix Content When Peptides Are Inserted into Phosphatidylserine Vesicles

The secondary structures of the peptides used above were evaluated by circular dichroism. Secondary structure was evaluated at different pH values and in different lipid compositions (Table 3). In all cases, the peptides had a largely helical structure. In the presence of DOPC vesicles, helix content was generally in the range 65-75%, which corresponds to helix formation by almost all of the residues in the hydrophobic core of the peptides. The more weakly hydrophobic peptides exhibited a helix content at the lower end of this range. For Asp-containing peptides helix content in DOPC vesicles was not greatly affected by whether a peptide formed a TM state (at low pH) or non-TM state (at high pH). There was also little dependence of helix content upon lipid composition, with the striking exception of DOPS

vesicles, in which there was an increase in helix content to 80-90%. Because DOPG vesicles did not induce a significant increase in helix content, this increase cannot be due simply to DOPS being anionic (see Discussion).

DISCUSSION

Role of Negative Lipid in TM Stability: Electrostatic Interactions

It is well known that, relative to zwitterionic lipids, anionic lipids enhance the binding of cationic polypeptides to membranes[36,37]. The results in this report demonstrate that anionic lipids also stabilize the TM topography of hydrophobic α-helices with flanking cationic residues relative to the non-TM topography. This is not simply a matter of enhanced binding to the membrane, because an enhancement of the amount of peptide in a TM state by anionic lipid is observed in cases in which a peptide is fully bound to zwitterionic vesicles. Thus, there are two effects of anionic lipids upon polypeptide-membrane interaction, as summarized in Figure 8A.

Several lines of evidence are consistent with this being a result of Coulombic type electrostatic interactions. First, stabilization depends on lipid having a negative charge and peptide having a positive charge. Second, stabilization of the TM state is observed with more than one type of anionic lipid. Third, stabilization is not specific for the type of charged residue. Finally, the effect increases with the number of positive charges on the peptide, as shown by the observation that stabilization of TM topography was greater when there were two flanking positive charges than when there was one flanking positive charge.

Presumably, interactions between positively charged residues and anionic lipid head groups decrease the free energy of the peptides in the TM state relative to that when the bilayer is uncharged. However, the free energy of a membrane-bound non-TM state should also be decreased by electrostatic interactions. The TM topography may be preferentially stabilized because cationic residues are further from the hydrophobic core of the bilayer in the non-TM state than when in the TM state, so that the electrostatic interactions stabilize the free energy of the non-TM state to a lesser degree than they do that of the TM state.

The electrostatic interaction between peptide and lipid is probably stronger than in bulk aqueous solution because charged amino acid residues located near or at the boundary between the non-polar/polar regions of the bilayer should experience a local environment with a lower effective dielectric coefficient than in bulk water. Consistent with this, it has been reported that free energy is higher for charged residues near the membrane bilayer in ER translocon system[4,38].

The degree of stabilization of the TM state by anionic lipid is substantial. Assuming that when a peptide appears to be fully in the non-TM state in DOPC it is only 90% non-TM and fully-TM in DOPS only corresponds to 90% TM, gives a lower limit to the effect $\Delta\Delta G°$ TM/non-TM in DOPS relative to DOPC of close to 3 kcal/mole. This is a crude estimation and could easily be half or even less of the true $\Delta\Delta G°$.

It should be noted that hydrophobic peptides that equilibrate between fully soluble and fully TM states may be useful for evaluating the effect of different residues upon the relative stability of these two states via experiments in which various substitutions are made in these sequences. This could provide a hydrophobicity scale that would complement other types of scales, and which would be particularly useful for biological cases in which there is post-translational equilibration of hydrophobic sequences between TM and soluble states.

The Origin of the Difference Between Peptide Topography in DOPS and DOPG

One of the most striking observations in this report was that there was a substantial difference between peptide topography in DOPS vesicles and DOPG vesicles. This is an interesting observation because the functional significance of the different types of anionic phospholipids is a long standing mystery in biology. The difference between DOPG and DOPS vesicles is puzzling in terms of a simple electrostatic interaction. Both PG and PS should have a net -1 charge on their polar headgroups at the experimental pH studied. However, PS has two negative charges, one on the phosphate and one on the carboxyl, and one possibility is that the PS headgroup can orient so as to allow both charges to interact with cationic residues. Another possibility is that differences in hydrogen bonding or other polar interactions between peptide and lipid are affected by the difference in PS and PG headgroup structure. Studies have shown that changes in lipid composition that affect the dipoles near the interfacial region can disrupt the binding of helical peptides to a lipid bilayer[39].

The nature of the difference in polypeptide topography in DOPS and DOPG vesicles is also of interest. As noted in the results, the fluorescence behavior for peptides in which topography in DOPS and DOPG was compared does not fit a model in which topography in DOPG is simply explained by the presence of a co-existing TM state similar to that in DOPS vesicles and a non-TM state similar to that in DOPC vesicles. An alternative that does fit the data is that there are two different TM states in DOPS and DOPG vesicles which differ in the degree of positional anchoring of the TM helix. We have previously proposed that in the absence of heteroaromatic residues at the boundary of the hydrophobic sequence, decreasing TM peptide core hydrophobicity (by substituting Leu with Ala) decreases anchoring of the sequence at a precise position in membranes, such that there is decreased burial of one or the other end of the hydrophobic core of the peptide within the bilayer[28]. A greater degree of peptide anchoring in DOPS vesicles could also explain the difference between peptide behavior in DOPG and DOPS vesicles (Figure 8B). Notice that, as illustrated in Figure 8, a loss of precise anchoring would be associated with a shallower Trp depth, consistent with the shallower Trp depth observed in DOPG vesicles. This model is also consistent with the observation of less helical structure in DOPG vesicles than in DOPS vesicles. A poorly-anchored hydrophobic sequence would have additional residues exposed to aqueous solution, and such residues would not need to be constrained in a helical structure. It should be noted that sensitivity of anchoring to lipid structure might be sequence dependent. Heteroaromatic residues have a distinct energetic preference for the polar/non-polar boundary of the bilayer[4,38,40,41] and their presence at the end of the hydrophobic segment might compensate for anchoring that would otherwise be weak. In any case, our report points to cationic residue-PS interaction as a novel factor controlling TM peptide anchoring, and worthy of further study.

The hydrophobicity of the core sequence may also be important for determining how well a TM state is anchored. Trp location for the $^{KK}pL_7A_8$(D10) peptide as DOPG levels in the membrane increased was found to plateau at a depth that was shallower than observed for the peptides with a more hydrophobic (Leu-rich) core. This is consistent with the idea that the unfavorable energetics of exposing Leu in the latter peptides to aqueous solution, relative to the cost of exposing Ala, also anchors the TM topography in a constant position relative to the bilayer.

A second, but less likely possibility for the shallow Trp depths observed for peptides in DOPG vesicles relative to in DOPS is that there is greater stabilization of the TM state in DOPS vesicles than in DOPG vesicles, but that the stabilization is not easily detected by fluorescence. It is possible that when incorporated into DOPG vesicles the Trp residue in the non-TM state locates more deeply than when incorporated into vesicle lacking a net charge, so that there is only a moderate difference between Trp depth in the TM and non-TM states, and their coexistence cannot be detected easily via quencher-induced λmax shifts. It is also possible that

a relatively deeply penetrating non-TM state co-exists with the poorly anchored TM state described above, and these two states might have similar average Trp depths.

Effect of POPE and Cholesterol upon the Stability of the Surface Bound Non-TM Topography

Cholesterol and POPE appeared to disfavor the surface associated non-TM state relative to the state in which the peptides are dissolved in solution. A possible explanation arises from the fact that cholesterol and POPE have headgroups that are smaller than those of other lipids, so that they may pack more tightly in the headgroup region of the bilayer. This can affect bilayer physical properties like compressibility and spontaneous lipid curvature in a fashion that tends to inhibit binding of peptides to membranes[42-47].

Physiological Significance of Stabilization of TM Topography by Negatively Charged Lipids

Electrostatic interactions between anionic lipids and cationic residues have important biological consequences. The preferential interaction of water soluble positively charged peptides and peripheral proteins with anionic lipids has been extensively characterized in numerous cases[36,37,48]. Antimicrobial peptides, which are generally cationic, are believed to disrupt the microbial membrane by interacting with negatively charged lipids[49,50]. Preferential interactions between sites on TM proteins and anionic lipids have also been documented, and the anionic lipid may often have an important structural and functional role[51-55]. There is already evidence that anionic lipids affect TM protein orientation in cells. In cell membrane, TM helices orient such that the more cationic of their flanking hydrophilic sequences tends to orient towards the cytoplasmic surface of membrane (positive-inside rule), and studies have found that anionic phospholipids control orientation by what appears to be an electrostatic interaction with cationic residues[56,57].

In this regard, the ability of DOPS to promote helix formation may be important for determining peptide behavior in DOPS vesicles and in real membranes. It is interesting to note that the ability of cationic residues on the cytofacial side of the membrane to form a helical continuation of a hydrophobic helix structure has been shown to be important for the formation of a TM topography during membrane insertion in the translocon[38]. The cytofacial surface of the endoplasmic reticulum membrane presumably contains a significant amount of PS, and thus PS might play a role in this process.

Stabilization of the TM state by anionic lipids may be particularly important for proteins that undergo post-translational changes in topography. As noted in the introduction, a number of proteins have hydrophobic sequences that post-translationally convert from a non-TM to TM state. Stabilization of the TM state might be most important for determining the structure of the hydrophobic sequences in such proteins when they are semi-hydrophobic, i.e. have a hydrophobicity at the borderline necessary for stability in the TM state. For example, although several studies have shown polyAla sequences do not form stable TM helices in vitro[19,35,58,59], the results in our study suggest this would not necessarily be the case in natural membranes containing moderate amounts of anionic lipids. Other sequences with borderline hydrophobicity may not be rare. Genomic analysis has revealed that there are numerous semi-hydrophobic sequences with borderline hydrophobicity in both prokaryotes and eukaryotes[60].

Furthermore, TM state stabilizing effects were observed at levels of anionic lipid ($\leq$20%) within the physiological level believed to be present on the cytofacial leaflet. It should be interesting in future studies to investigate the effect of anionic lipids upon membrane proteins with natural semi-hydrophobic sequences in order to determine whether anionic lipids, and/or the type of anionic lipid present, have a significant effect on topography.

Materials and Methods

Materials

Peptides: Acetyl-$K_2L_7DWL_8K_2$-amide [$^{KK}pL_{15}$(D10)], $K_2LAL_5DWL_6ALK_2$-amide [$^{KK}pL_{13}A_2$(D10)], acetyl-$K_2(LA)_2L_3DWL_4(AL)_2K_2$-amide [$^{KK}pL_{11}A_4$(D10)], acetyl-$K_2(LA)_3LDWL_2(AL)_3K_2$-amide [$^{KK}pL_9A_6$(D10)], acetyl-$K_2(LA)_3ADW(AL)_4K_2$-amide [$^{KK}pL_7A_8$(D10)], acetyl-$K_2GL_6WL_6K_2A$-amide [$^{KK}pL_{12}$], acetyl-$KHGL_6WL_6HKA$-amide [$^{KH}pL_{12}$], acetyl-$H_2L_6WL_6H_2$-amide [$^{HH}pL_{12}$], acetyl-$K_2A_9WA_9K_2$-amide [$^{KK}pA_{18}$], acetyl-$R_2A_9WA_9R_2$-amide [$^{RR}pA_{18}$], acetyl-$K_2LA_9LWLA_9LK_2$-amide [$^{KK}pL_4A_{18}$], acetyl-$K_4(LA)_2L_3DWL_4(AL)_2K_4$-amide [$^{KKKK}pL_{11}A_4$(D10)], acetyl-$K_2LA_9WA_9LK_2$-amide [$^{KK}pL_2A_{18}$] and acetyl-$K_2A_{11}WA_{11}K_2$-amide [$^{KK}pA_{22}$] were purchased from Anaspec Inc. (San Jose, CA). (Notice that the peptide names do not include the Trp at the center of the hydrophobic sequence.) The peptides were purified via reversed-phase HPLC using a C18 column using a 2-propanol/water gradient containing 0.5% (v/v) trifluoroacetic acid as described previously[61]. The peptides were dried under N_2, redissolved in 1:1 (v/v) 2-propanol/water, and stored at 4°C. Peptide purity was confirmed by MALDI-TOF (Proteomics Center, Stony Brook University) and generally was ~90% or greater. Estimated purity was lower (about 80%) only for $^{KK}pL_{11}A_4$(D10) and $^{KK}pL_9A_6$(D10). The concentrations of purified peptides were measured by absorbance spectroscopy using a Beckman DU-650 spectrophotometer, using an ε for Trp of 5560 M^{-1} cm^{-1} at 280 nm. Phosphatidylcholines (1,2-diacyl-*sn*-glycero-3-phosphocholines), [diC14:1Δ9cPC (dimyristoleoylphosphatidylcholine); diC16:1Δ9cPC; diC18:1Δ9cPC, (dioleoylphosphatidylcholine, DOPC); diC20:1Δ11cPC; diC22:1Δ13cPC, (dierucoylphosphatidylcholine); and diC24:1Δ15cPC; 1,2-dioleoyl-*sn*-glycero-3-[phospho-L-serine] sodium salt (DOPS), 1,2-dioleoyl-*sn*-glycero-3-[phospho-*rac*-(1-glycerol)] sodium salt (DOPG), 1-palmitoyl-2-oleoyl-*sn*-glycero-3-phosphoethanolamine (POPE), 1-palmitoyl-2-oleoyl-*sn*-glycero-3-phosphocholine (POPC) and cholesterol were purchased from Avanti Polar Lipids (Alabaster, AL). Lipids were stored in chloroform at -20°C. Lipid concentrations were determined by dry weight. Acrylamide was purchased from Sigma-Aldrich Chemical Co. (St. Louis, MO). 10-doxylnonadecane (10-DN) was custom-synthesized (contact authors for availability) by Molecular Probes (Eugene, OR). It was stored as a 6 mM stock solution [determined using ε= 12 M^{-1} cm^{-1} at 422 nm[29]in ethanol at -20°C.

Model Membrane Vesicle Preparation

Model membranes were prepared using the ethanol-dilution method[25,26]. Peptides dissolved in 1:1 (v/v) 2-propanol/water and lipids dissolved in chloroform were mixed and then dried under a stream of N_2. Samples were then further dried under high vacuum for 1h. Then, 10 μL (for 800 μL samples) or 30 μL (for 2 mL samples) of 100% ethanol was added to dissolve the dried peptide/lipid film. To disperse the lipid-peptide mixtures 790 or 1970 μL, respectively, of PBS (10 mM sodium phosphate and 150 mM NaCl, pH 7), was added to the samples while vortexing. For samples prepared at low or high pH, the pH of the PBS was first adjusted using glacial acetic acid, for pH 3.8-5.5, or 2 M NaOH, for pH 9.0. The final concentrations were 2 μM peptide and 200 μM lipid, except for pH titration experiments using peptides incorporated into DOPS vesicles in which, due to the difficulty of dissolving DOPS in ethanol, the final concentrations used were 1 μM peptide and 100 μM lipid.

Fluorescence Measurements

Fluorescence data were obtained on a SPEX τ2 Fluorolog spectrofluorometer operating in steady-state mode. Measurements were taken on samples in semimicro quartz cuvettes (1-cm excitation path length and 4-mm emission path length), except in the titration experiments, in which a 1-cm excitation and 1-cm emission path-length cuvette was used. A 2.5-mm excitation slit width and 5-mm emission slit width (band pass of 4.5 and 9 nm, respectively) were used for all experiments. Trp fluorescence emission spectra were measured over the range of

300-375 nm. Fluorescence from background samples containing lipid but lacking peptide was subtracted from the reported values. All measurements were made at room temperature.

pH Titration Experiments

As described above, 2 mL samples containing peptide incorporated into vesicles were prepared using PBS adjusted to about pH 4, and their Trp fluorescence emission intensity was measured at 330 and 350 nm. Sample pH was increased by adding 1-8 μL aliquots of either 0.25 or 2 M NaOH. After each aliquot was added and the sample mixed, it was incubated for 2 min (control experiments show this to be a sufficient time for equilibration of pH across the bilayer[5,62] and then fluorescence was remeasured. The total volume of NaOH added by the end of the titration experiment (by which pH was 11.4-11.6) was about 70 μL. Intensities were corrected for background fluorescence using control samples lacking peptide. The pH dependence of the ratio of fluorescence intensity at 350 nm and 330 nm (F_{350}/F_{330}) was calculated. The data was fitted to a sigmoidal curve (Slidewrite Program, Advanced Graphics Solutions, Encinitas, CA), and apparent pKa values were estimated from the pH at the inflection point of the F_{350}/F_{330} ratio vs. pH curve. Distortions of the apparent pKa due to a change in Trp quantum yield upon peptide deprotonation was small (≤0.2 pH units, see Supplemental Figure S1).

Acrylamide Quenching Measurements

Fluorescence intensity and emission spectra were first measured for model membrane-incorporated peptides or background samples. After addition of a 50 μL aliquot of acrylamide from a 4 M stock solution in water and a 5min incubation period, fluorescence was remeasured. (This is sufficient time for acrylamide to equilibrate across the bilayer[29].) Fluorescence intensity was measured at an excitation wavelength of 295 nm and an emission wavelength of 340 nm. This excitation wavelength was chosen to reduce the resulting inner filter effect due to acrylamide absorbance. Corrections to intensity were made both for dilution by the addition of acrylamide and for the residual inner filter effects[29]. Fluorescence emission spectra were recorded using an excitation wavelength of 280 nm, despite the stronger inner-filter effect arising from acrylamide at 280 nm, because the overall intensity was greater than when an excitation wavelength of 295 nm was used. Controls show that emission spectra have very similar wavelength maxima using either excitation wavelength[29].

10-DN-Quenching Measurements

To measure quenching in samples containing 10mol% 10-DN, samples containing model membrane-incorporated peptides or background samples without peptide were prepared in which 10 mol % of each of the lipids present was replaced by an equivalent mole fraction of 10-DN. Fluorescence intensity and emission spectra were measured for samples with and without 10-DN. Fluorescence intensity was measured using an excitation wavelength of 280 nm and an emission wavelength of 330 nm. Emission spectra were recorded using an excitation wavelength of 280 nm.

Calculation of the Acrylamide/10-DN Quenching Ratio (Q Ratio)

The ratio of quenching by acrylamide to quenching by 10-DN was used to estimate Trp depth in the bilayer. This ratio was calculated from the formula Q ratio = [(F_o/F acrylamide) - 1]/[($F_o/F_{10\text{-DN}}$) - 1], where F_o is the fluorescence of the sample with no quencher present and $F_{\text{acrylamide}}$ and $F_{10\text{-DN}}$ are the fluorescence intensities in the presence of acrylamide or 10-DN, respectively[29].

Circular Dichroism (CD) Measurements

Circular dichroism spectra were recorded on a Jasco J-715 CD spectrophotometer at room temperature using a 1-mm path-length quartz cuvette. Unless otherwise noted, samples were

prepared using 5 μM or 10μM peptide and 500μM lipid. The spectra were obtained from at least 50 scans. Backgrounds from samples lacking peptide were subtracted. Overall α-helix content was estimated using CONTINLL deconvolution program.

Supplementary Material

Refer to Web version on PubMed Central for supplementary material.

Acknowledgements

Supported by NIH Grant GM 48596

References

1. Aires JR, Pechere JC, Van Delden C, Kohler T. Amino acid residues essential for function of the MexF efflux pump protein of Pseudomonas aeruginosa. Antimicrob Agents Chemother 2002;46:2169–2173. [PubMed: 12069970]
2. Subramaniam S, Greenhalgh DA, Khorana HG. Aspartic acid 85 in bacteriorhodopsin functions both as proton acceptor and negative counterion to the Schiff base. J Biol Chem 1992;267:25730–25733. [PubMed: 1464589]
3. Caputo GA, London E. Cumulative effects of amino acid substitutions and hydrophobic mismatch upon the transmembrane stability and conformation of hydrophobic alpha-helices. Biochemistry 2003;42:3275–3285. [PubMed: 12641459]
4. Hessa T, White SH, von Heijne G. Membrane insertion of a potassium-channel voltage sensor. Science 2005;307:1427. [PubMed: 15681341]
5. Lew S, Ren J, London E. The effects of polar and/or ionizable residues in the core and flanking regions of hydrophobic helices on transmembrane conformation and oligomerization. Biochemistry 2000;39:9632–9640. [PubMed: 10933779]
6. Kachel K, Ren J, Collier RJ, London E. Identifying transmembrane states and defining the membrane insertion boundaries of hydrophobic helices in membrane-inserted diphtheria toxin T domain. J Biol Chem 1998;273:22950–22956. [PubMed: 9722516]
7. Wang Y, Malenbaum SE, Kachel K, Zhan H, Collier RJ, London E. Identification of shallow and deep membrane-penetrating forms of diphtheria toxin T domain that are regulated by protein concentration and bilayer width. J Biol Chem 1997;272:25091–25098. [PubMed: 9312118]
8. Petosa C, Collier RJ, Klimpel KR, Leppla SH, Liddington RC. Crystal structure of the anthrax toxin protective antigen. Nature 1997;385:833–838. [PubMed: 9039918]
9. Tilley SJ, Orlova EV, Gilbert RJ, Andrew PW, Saibil HR. Structural basis of pore formation by the bacterial toxin pneumolysin. Cell 2005;121:247–256. [PubMed: 15851031]
10. Shepard LA, Heuck AP, Hamman BD, Rossjohn J, Parker MW, Ryan KR, Johnson AE, Tweten RK. Identification of a membrane-spanning domain of the thiol-activated pore-forming toxin Clostridium perfringens perfringolysin O: an alpha-helical to beta-sheet transition identified by fluorescence spectroscopy. Biochemistry 1998;37:14563–14574. [PubMed: 9772185]
11. Antignani A, Youle RJ. How do Bax and Bak lead to permeabilization of the outer mitochondrial membrane? Curr Opin Cell Biol 2006;18:685–689. [PubMed: 17046225]
12. Wattenberg B, Lithgow T. Targeting of C-terminal (tail)-anchored proteins: understanding how cytoplasmic activities are anchored to intracellular membranes. Traffic 2001;2:66–71. [PubMed: 11208169]
13. Fujita K, Krishnakumar SS, Franco D, Paul AV, London E, Wimmer E. Membrane topography of the hydrophobic anchor sequence of poliovirus 3A and 3AB proteins and the functional effect of 3A/3AB membrane association upon RNA replication. Biochemistry 2007;46:5185–5199. [PubMed: 17417822]
14. Huang HW. Molecular mechanism of antimicrobial peptides: the origin of cooperativity. Biochim Biophys Acta 2006;1758:1292–1302. [PubMed: 16542637]

15. Wang X, Bogdanov M, Dowhan W. Topology of polytopic membrane protein subdomains is dictated by membrane phospholipid composition. EMBO J 2002;21:5673–5681. [PubMed: 12411485]
16. Xie J, Bogdanov M, Heacock P, Dowhan W. Phosphatidylethanolamine and monoglucosyldiacylglycerol are interchangeable in supporting topogenesis and function of the polytopic membrane protein lactose permease. J Biol Chem 2006;281:19172–19178. [PubMed: 16698795]
17. Giddings KS, Johnson AE, Tweten RK. Redefining cholesterol's role in the mechanism of the cholesterol-dependent cytolysins. Proc Natl Acad Sci USA 2003;100:11315–11320. [PubMed: 14500900]
18. Bechinger B. Towards membrane protein design: pH-sensitive topology of histidine-containing polypeptides. J Mol Biol 1996;263:768–775. [PubMed: 8947574]
19. Bechinger B. Membrane insertion and orientation of polyalanine peptides: a (15)N solid-state NMR spectroscopy investigation. Biophys J 2001;81:2251–2256. [PubMed: 11566795]
20. Killian JA. Hydrophobic mismatch between proteins and lipids in membranes. Biochim Biophys Acta 1998;1376:401–415. [PubMed: 9805000]
21. Killian JA, Nyholm TK. Peptides in lipid bilayers: the power of simple models. Curr Opin Struct Biol 2006;16:473–479. [PubMed: 16828281]
22. van Duyl BY, Meeldijk H, Verkleij AJ, Rijkers DT, Chupin V, de Kruijff B, Killian JA. A synergistic effect between cholesterol and tryptophan-flanked transmembrane helices modulates membrane curvature. Biochemistry 2005;44:4526–4532. [PubMed: 15766283]
23. Liu F, Lewis RN, Hodges RS, McElhaney RN. Effect of variations in the structure of a polyleucine-based alpha-helical transmembrane peptide on its interaction with phosphatidylethanolamine Bilayers. Biophys J 2004;87:2470–2482. [PubMed: 15454444]
24. Lewis RN, Liu F, Krivanek R, Rybar P, Hianik T, Flach CR, Mendelsohn R, Chen Y, Mant CT, Hodges RS, McElhaney RN. Studies of the minimum hydrophobicity of alpha-helical peptides required to maintain a stable transmembrane association with phospholipid bilayer membranes. Biochemistry 2007;46:1042–1054. [PubMed: 17240988]
25. Ren J, Lew S, Wang Z, London E. Transmembrane orientation of hydrophobic alpha-helices is regulated both by the relationship of helix length to bilayer thickness and by the cholesterol concentration. Biochemistry 1997;36:10213–10220. [PubMed: 9254619]
26. Ren J, Lew S, Wang J, London E. Control of the transmembrane orientation and interhelical interactions within membranes by hydrophobic helix length. Biochemistry 1999;38:5905–5912. [PubMed: 10231543]
27. Krishnakumar SS, London E. The control of transmembrane helix transverse position in membranes by hydrophilic residues. J Mol Biol 2007;374:1251–1269. [PubMed: 17997412]
28. Krishnakumar SS, London E. Effect of sequence hydrophobicity and bilayer width upon the minimum length required for the formation of transmembrane helices in membranes. J Mol Biol 2007;374:671–687. [PubMed: 17950311]
29. Caputo GA, London E. Using a novel dual fluorescence quenching assay for measurement of tryptophan depth within lipid bilayers to determine hydrophobic alpha-helix locations within membranes. Biochemistry 2003;42:3265–3274. [PubMed: 12641458]
30. Tsui FC, Ojcius DM, Hubbell WL. The intrinsic pKa values for phosphatidylserine and phosphatidylethanolamine in phosphatidylcholine host bilayers. Biophys J 1986;49:459–468. [PubMed: 3955180]
31. MacDonald RC, Simon SA, Baer E. Ionic influences on the phase transition of dipalmitoylphosphatidylserine. Biochemistry 1976;15:885–891. [PubMed: 2290]
32. Maltseva E, Shapovalov VL, Mohwald H, Brezesinski G. Ionization state and structure of l-1,2-dipalmitoylphosphatidylglycerol monolayers at the liquid/air interface. J Phys Chem B 2006;110:919–926. [PubMed: 16471624]
33. Koynova R, Caffrey M. Phases and phase transitions of the phosphatidylcholines. Biochim Biophys Acta 1998;1376:91–145. [PubMed: 9666088]
34. Caputo GA, London E. Position and ionization state of Asp in the core of membrane-inserted alpha helices control both the equilibrium between transmembrane and nontransmembrane helix

topography and transmembrane helix positioning. Biochemistry 2004;43:8794–8806. [PubMed: 15236588]

35. Hammond K, Caputo GA, London E. Interaction of the membrane-inserted diphtheria toxin T domain with peptides and its possible implications for chaperone-like T domain behavior. Biochemistry 2002;41:3243–3253. [PubMed: 11863463]
36. Liu LP, Deber CM. Anionic phospholipids modulate peptide insertion into membranes. Biochemistry 1997;36:5476–5482. [PubMed: 9154930]
37. Lad MD, Birembaut F, Clifton LA, Frazier RA, Webster JR, Green RJ. Antimicrobial peptide-lipid binding interactions and binding selectivity. Biophys J 2007;92:3575–3586. [PubMed: 17325007]
38. Hessa T, Meindl-Beinker NM, Bernsel A, Kim H, Sato Y, Lerch-Bader M, Nilsson I, White SH, von Heijne G. Molecular code for transmembrane-helix recognition by the Sec61 translocon. Nature 2007;450:1026–1030. [PubMed: 18075582]
39. Voglino L, McIntosh TJ, Simon SA. Modulation of the binding of signal peptides to lipid bilayers by dipoles near the hydrocarbon-water interface. Biochemistry 1998;37:12241–12252. [PubMed: 9724538]
40. Kachel K, Asuncion-Punzalan E, London E. Anchoring of tryptophan and tyrosine analogs at the hydrocarbon-polar boundary in model membrane vesicles: parallax analysis of fluorescence quenching induced by nitroxide-labeled phospholipids. Biochemistry 1995;34:15475–15479. [PubMed: 7492549]
41. Yau WM, Wimley WC, Gawrisch K, White SH. The preference of tryptophan for membrane interfaces. Biochemistry 1998;37:14713–14718. [PubMed: 9778346]
42. Egashira M, Gorbenko G, Tanaka M, Saito H, Molotkovsky J, Nakano M, Handa T. Cholesterol modulates interaction between an amphipathic class A peptide, Ac-18A-NH2, and phosphatidylcholine bilayers. Biochemistry 2002;41:4165–4172. [PubMed: 11900560]
43. Saito H, Miyako Y, Handa T, Miyajima K. Effect of cholesterol on apolipoprotein A-I binding to lipid bilayers and emulsions. J Lipid Res 1997;38:287–294. [PubMed: 9162748]
44. Allende D, Simon SA, McIntosh TJ. Melittin-induced bilayer leakage depends on lipid material properties: evidence for toroidal pores. Biophys J 2005;88:1828–1837. [PubMed: 15596510]
45. Lewis JR, Cafiso DS. Correlation between the free energy of a channel-forming voltage-gated peptide and the spontaneous curvature of bilayer lipids. Biochemistry 1999;38:5932–5938. [PubMed: 10231547]
46. McIntosh TJ, Simon SA. Roles of bilayer material properties in function and distribution of membrane proteins. Annu Rev Biophys Biomol Struct 2006;35:177–198. [PubMed: 16689633]
47. Evans, E. a. N., D. Physical properties of surfactant bilayer membrane:Thermal transitions, Elasticity, Rigidity, Cohesion, and Colloidal Interaction. J Phys Chem 1987;91:4219–4228.
48. Arbuzova A, Wang L, Wang J, Hangyas-Mihalyne G, Murray D, Honig B, McLaughlin S. Membrane binding of peptides containing both basic and aromatic residues. Experimental studies with peptides corresponding to the scaffolding region of caveolin and the effector region of MARCKS. Biochemistry 2000;39:10330–10339. [PubMed: 10956022]
49. Makovitzki A, Avrahami D, Shai Y. Ultrashort antibacterial and antifungal lipopeptides. Proc Natl Acad Sci USA 2006;103:15997–16002. [PubMed: 17038500]
50. Sitaram N, Nagaraj R. Interaction of antimicrobial peptides with biological and model membranes: structural and charge requirements for activity. Biochim Biophys Acta 1999;1462:29–54. [PubMed: 10590301]
51. Valiyaveetil FI, Zhou Y, MacKinnon R. Lipids in the structure, folding, and function of the KcsA K + channel. Biochemistry 2002;41:10771–10777. [PubMed: 12196015]
52. Gohil VM, Hayes P, Matsuyama S, Schagger H, Schlame M, Greenberg ML. Cardiolipin biosynthesis and mitochondrial respiratory chain function are interdependent. J Biol Chem 2004;279:42612–42618. [PubMed: 15292198]
53. Zhang M, Mileykovskaya E, Dowhan W. Cardiolipin is essential for organization of complexes III and IV into a supercomplex in intact yeast mitochondria. J Biol Chem 2005;280:29403–29408. [PubMed: 15972817]

54. Powl AM, East JM, Lee AG. Heterogeneity in the binding of lipid molecules to the surface of a membrane protein: hot spots for anionic lipids on the mechanosensitive channel of large conductance MscL and effects on conformation. Biochemistry 2005;44:5873–5883. [PubMed: 15823046]

55. Lee AG. How lipids and proteins interact in a membrane: a molecular approach. Mol Biosyst 2005;1:203–212. [PubMed: 16880984]

56. Heijne GV. The distribution of positively charged residues in bacterial inner membrane proteins correlates with the trans-membrane topology. EMBO J 1986;5:3021–3027. [PubMed: 16453726]

57. van Klompenburg W, Nilsson I, von Heijne G, de Kruijff B. Anionic phospholipids are determinants of membrane protein topology. EMBO J 1997;16:4261–4266. [PubMed: 9250669]

58. Nilsson I, Johnson AE, von Heijne G. How hydrophobic is alanine? J Biol Chem 2003;278:29389–29393. [PubMed: 12761228]

59. Lewis RN, Zhang YP, Hodges RS, Subczynski WK, Kusumi A, Flach CR, Mendelsohn R, McElhaney RN. A polyalanine-based peptide cannot form a stable transmembrane alpha-helix in fully hydrated phospholipid bilayers. Biochemistry 2001;40:12103–12111. [PubMed: 11580285]

60. Zhao G, London E. An amino acid “transmembrane tendency” scale that approaches the theoretical limit to accuracy for prediction of transmembrane helices: relationship to biological hydrophobicity. Protein Sci 2006;15:1987–2001. [PubMed: 16877712]

61. Lew S, London E. Simple procedure for reversed-phase high-performance liquid chromatographic purification of long hydrophobic peptides that form transmembrane helices. Anal Biochem 1997;251:113–116. [PubMed: 9300091]

62. Lew S, Caputo GA, London E. The effect of interactions involving ionizable residues flanking membrane-inserted hydrophobic helices upon helix-helix interaction. Biochemistry 2003;42:10833–10842. [PubMed: 12962508]

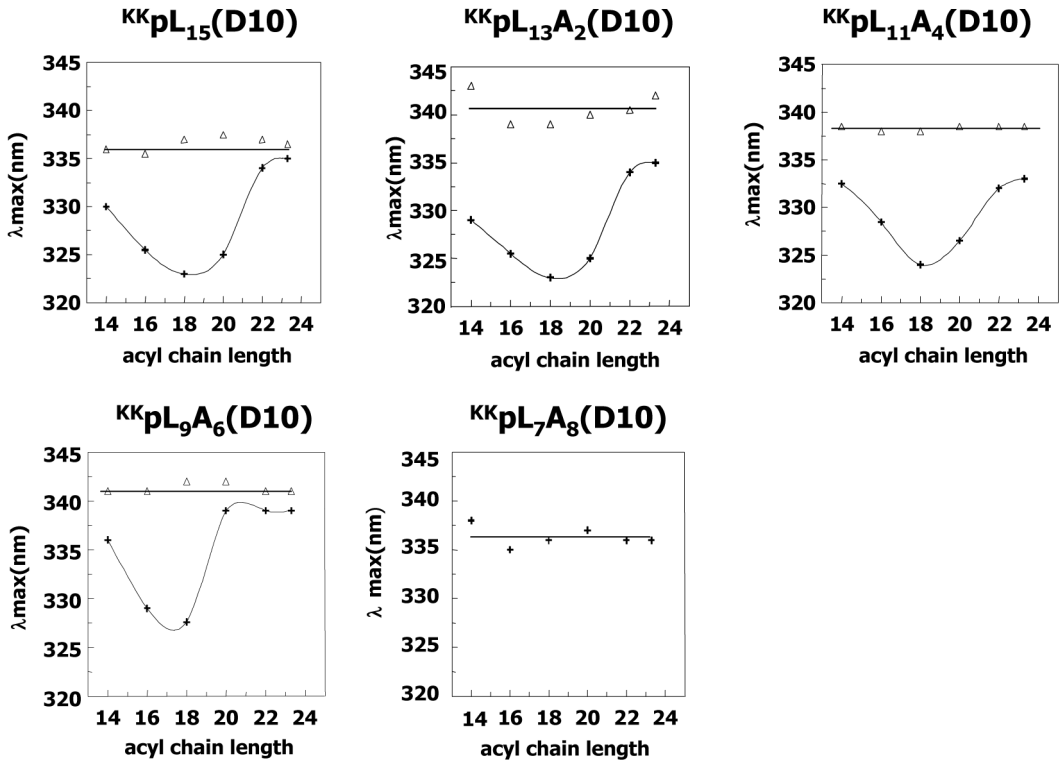

Figure 1.

Trp emission λmax of peptides incorporated into lipid vesicles composed of diunsaturated phosphatidylcholines with various (monounsaturated) acyl chain lengths. The vesicles were prepared at pH 3.8 (+) or 8.5 (Δ), values below and above the pKa of Asp residue, respectively. Samples in this and subsequent figures contained 2μM peptide and vesicles contained 200μM lipid unless otherwise noted. (A) $^{KK}pL_{15}(D10)$. (B) $^{KK}pL_{13}A_2(D10)$. (C) $^{KK}pL_{11}A_4(D10)$. (D) $^{KK}pL_9A_6(D10)$. (E) $^{KK}pL_7A_8(D10)$. In the case of $^{KK}pL_7A_8(D10)$ only the pH 3.8 curve is shown, as at pH 8.5 the peptide is not membrane bound and its λmax is off scale (350 –355 nm). The λmax values reported are average from at least three samples, and values for individual samples usually differ from the average value by no more than ±1 nm.

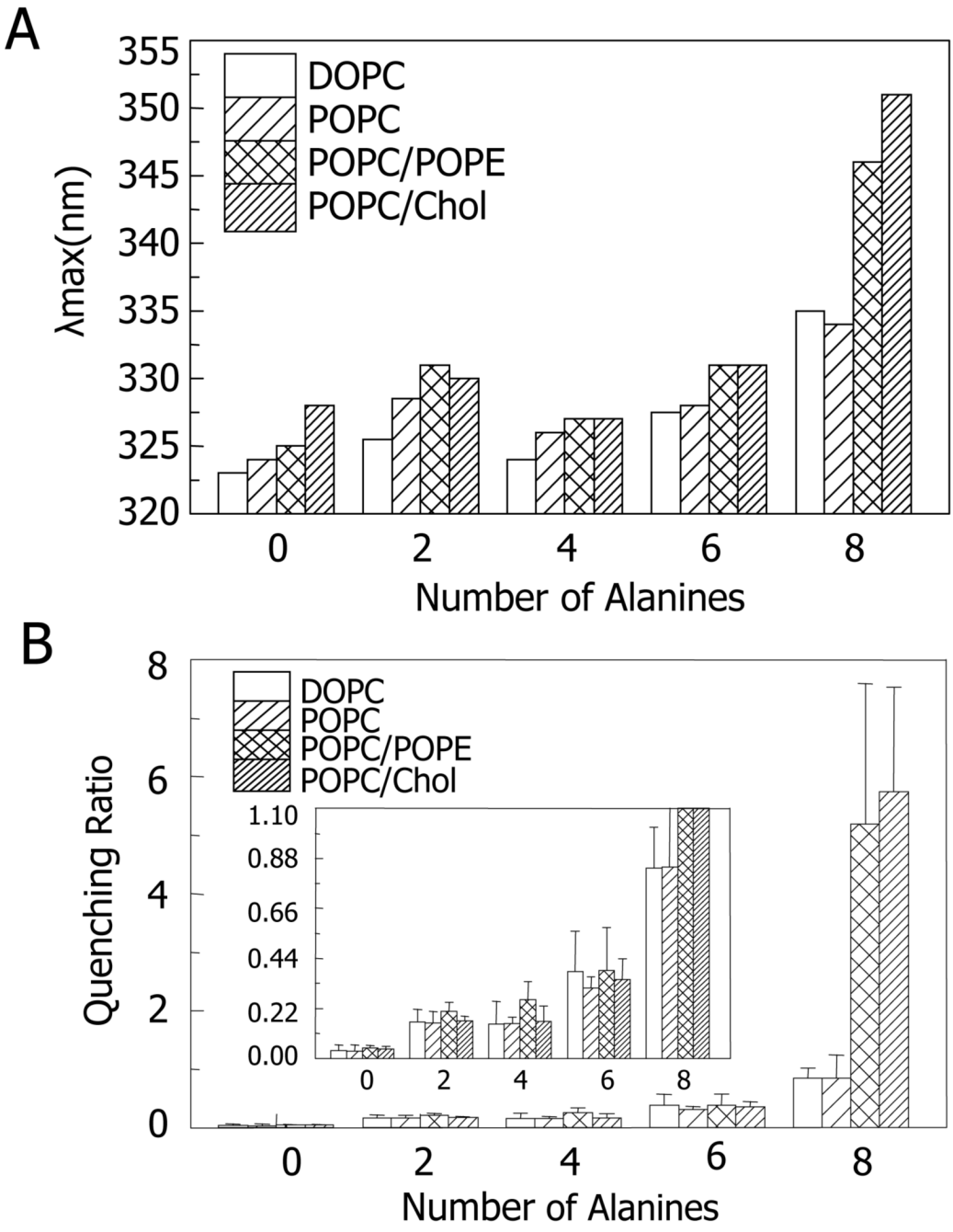

Figure 2.

Effect of lipid structure upon the stability of TM state measured by λmax and quenching ratio for peptides incorporated into lipid vesicles without net charge. (A) λmax. (B) Q-ratio. All samples were prepared at pH 4. POPC/POPE mol ratio is 1:1 and POPC/cholesterol mol ratio is 3:2. The λmax values and Q-ratio reported are average from at least three samples. Standard deviations for Q-ratios are shown and the λmax values in individual samples generally within ±1 nm of the average values. Inset: Version of (B) with expanded y-axis.

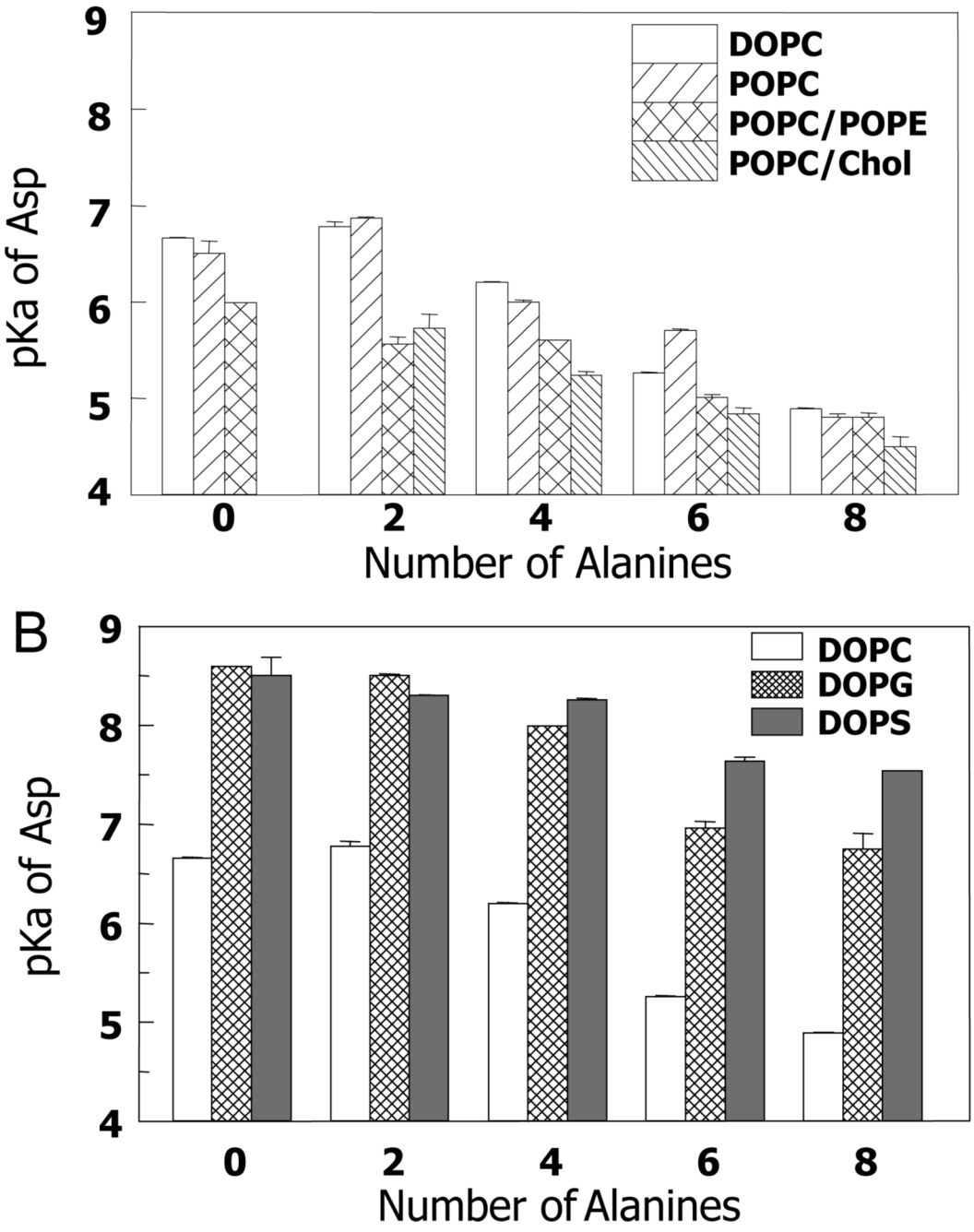

Figure 3.

Apparent Asp pKa of peptides in (A) Lipid vesicles with no net charge. (B) Lipid vesicles composed anionic lipids. (pKa values for DOPC vesicles are also shown in B. for purposes of comparison.) pKa values were estimated from the change in the ratio of fluorescence emission intensity at 330 nm to that at 350 nm as pH was increased in samples containing a 1:100 peptide:lipid mole ratio. Values shown are the average pKa from duplicates and their range. The pKa values have not been corrected for the difference in the quantum yield of Trp fluorescence when the peptide Asp is in the ionized and unionized states. Correcting for this variable does not shift pKa measured by more than ±0.2 units (see Supplemental Figure S1).

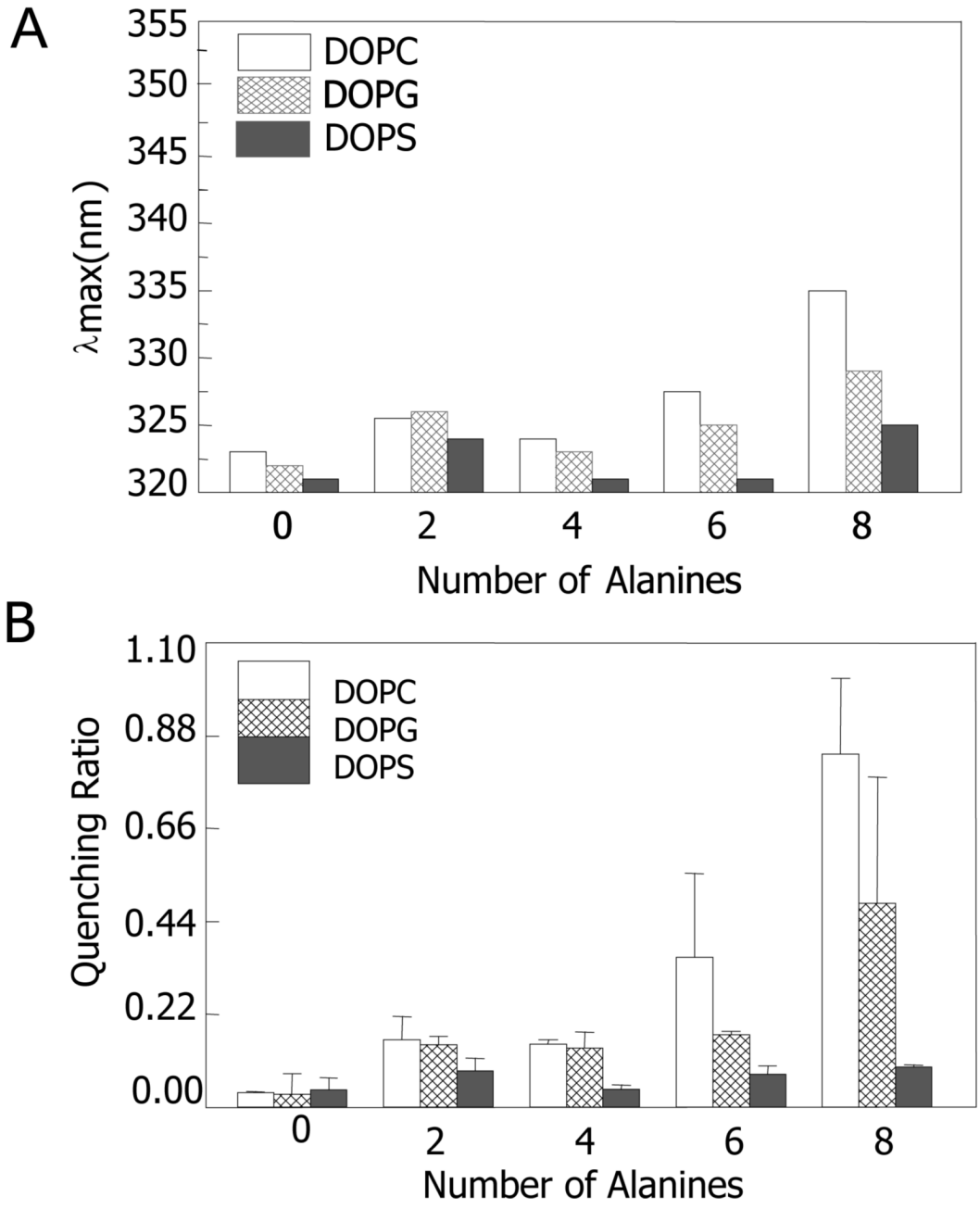

Figure 4.

Effect of lipid structure upon the stability of TM state measured by λmax and Q-ratio for peptides incorporated into anionic lipid vesicles. Values for the zwitterionic lipid DOPC are shown for comparison. (A) λmax. (B) Q-ratio. Samples were prepared at pH 4 except for those containing DOPS vesicles, which were prepared at pH 5.5 to maintain anionic charge on the PS headgroup. The results shown are for the average from three samples. Standard deviations are shown for Q-ratios. λmax values in individual samples were generally within ±1 nm of the average value.

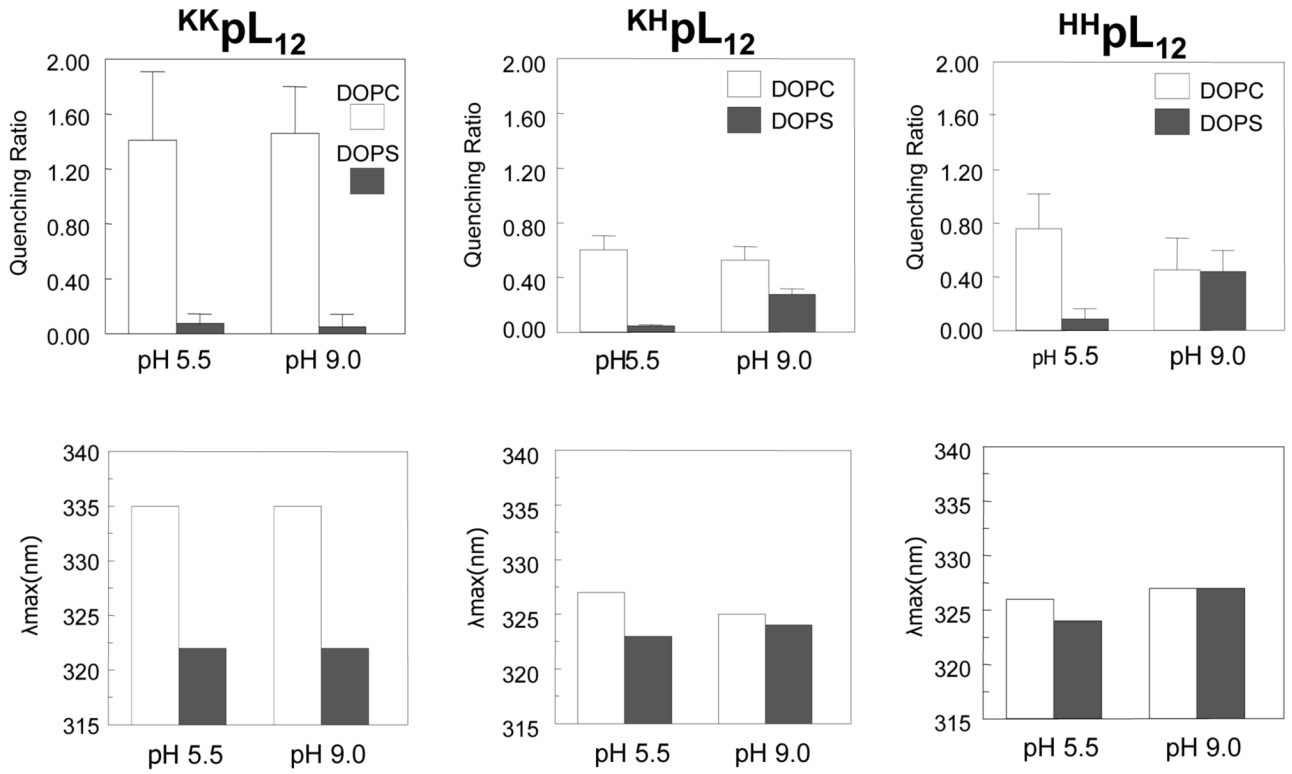

Figure 5.

Q-ratio and λmax for peptides with short hydrophobic sequences $^{KK}pL_{12}$, $^{HH}pL_{12}$, $^{KH}pL_{12}$ are shown when they are incorporated into vesicles composed of DOPC (open bars) or DOPS (filled bars) at pH 5.5 and pH 9.0. The results shown are for the average from three samples. Standard deviations are shown for Q-ratios. λmax values in individual samples were generally within ±1 nm of the average value.

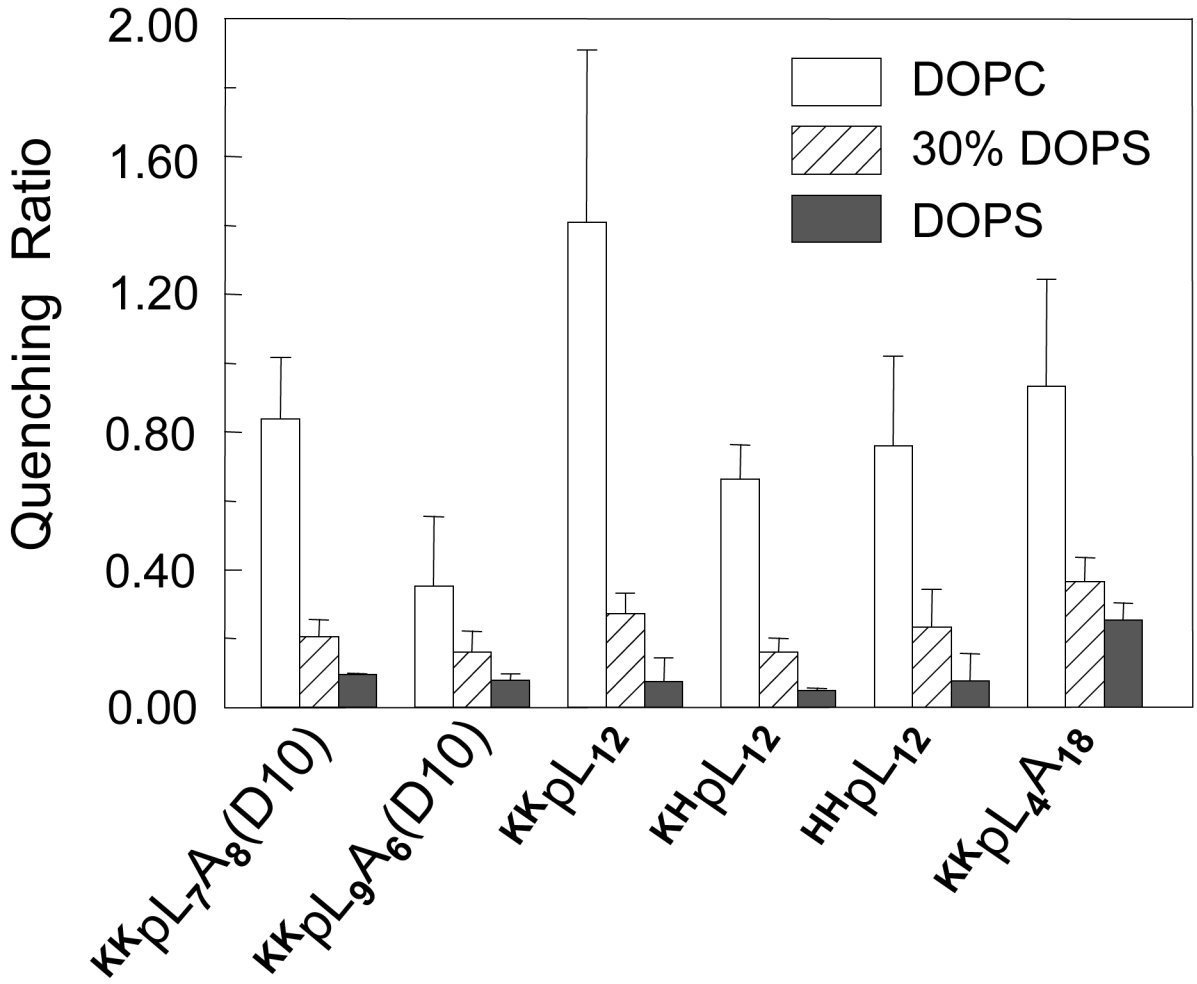

Figure 6.
Comparison of Q-ratio for peptides with different lengths and varying flanking residues in 30mol%DOPS/70mol%DOPC vesicles to that in pure DOPC or pure DOPS vesicles. Samples containing DOPS were prepared at pH 5.5; those containing only DOPC were prepared at pH 4.0. The results shown are for the average from three samples. Values shown are average from at least three samples and standard deviation.

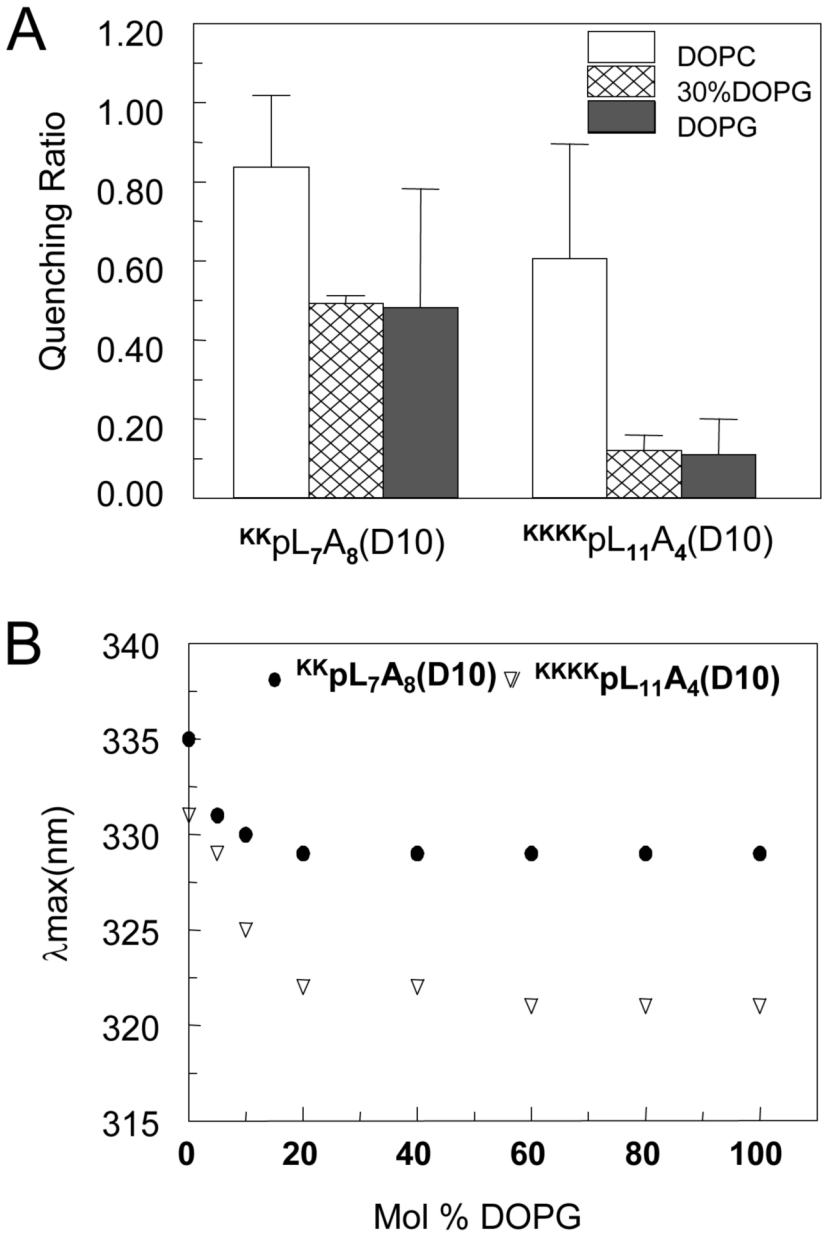

Figure 7.

Effect of the vesicle DOPG content upon Q-ratio and λmax for vesicle-associated $^{KKKK}pL_{11}A_4(D10)$ and $^{KK}pL_7A_8(D10)$ peptides. (A) Q-ratios at pH 4.0. Values reported are the average from at least three samples and standard deviation. (B)Trp emission λmax at pH 4.0. The results shown are for the average from two samples. λmax values in individual samples were generally within ±1 nm of the average value.

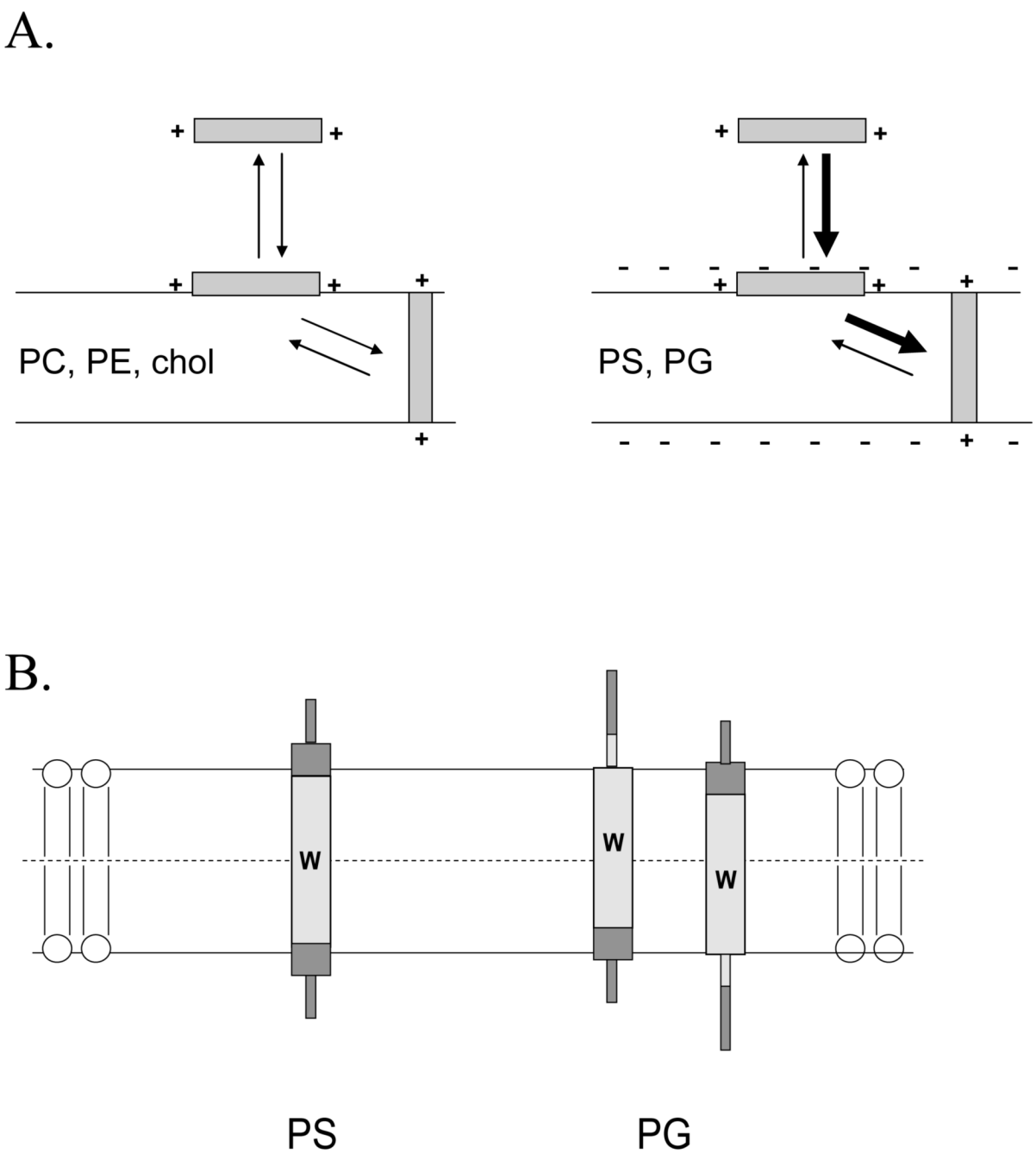

Figure 8.

Schematic illustration of the proposed difference in peptide topography in DOPG and DOPS-containing vesicles. (A) Effect of anionic lipid on membrane association and topographical equilibria. Notice that anionic lipid enhances both binding of polypeptides to membrane and the formation of the TM topography when the polypeptide is membrane-bound. (B) Difference between topography in DOPG and DOPS vesicles. Trp location is indicated by the “W”. The hydrophobic core of the peptide is shown by light gray shading and the hydrophilic flanking segments by dark gray shading. Helical sequences are indicated by thick rectangular regions and disordered sequences by thin rectangular regions. In addition to the topographical

difference illustrated here may be a lesser degree of formation of the TM topography in the presence of DOPG-containing vesicles.

Table 1

Sequences of the hydrophobic peptides used in this study. Notice that for simplicity the names do not explicitly mention the Trp at the center of the hydrophobic sequence.

Sequence	Name	Sequence
1	$^{KK}pL_{15}$(D10)	Acetyl-KKLLLLLLLDWLLLLLLLKK-amide
2	$^{KK}pL_{13}A_2$(D10)	Acetyl-KKLALLLLLDWLLLLLALK$_2$-amide
3	$^{KK}pL_{11}A_4$(D10)	Acetyl-KKLALALLLDWLLLLALALKK-amide
4	$^{KK}pL_9A_6$(D10)	Acetyl-KKLALALALDWLLALALALKK-amide
5	$^{KK}pL_7A_8$(D10)	Acetyl-KKLALALAADWALALALALKK-amide
6	$^{KKKK}pL_{11}A_4$(D10)	Acetyl-KKKKLALALLLDWLLLLALALKKKK-amide
7	$^{KK}pL_{12}$	Acetyl-KKGLLLLLLWLLLLLLKKA-amide
8	$^{KH}pL_{12}$	Acetyl-KHGLLLLLLWLLLLLLHKA-amide
9	$^{HH}pL_{12}$	Acetyl-HHLLLLLLWLLLLLLHH-amide
10	$^{KK}pA_{18}$	Acetyl-KKAAAAAAAAAWAAAAAAAAAK2-amide
11	$^{RR}pA_{18}$	Acetyl-RRAAAAAAAAAWAAAAAAAAALRR-amide
12	$^{KK}pL_2A_{18}$	Acetyl-KKLAAAAAAAAAWAAAAAAAAALK2-amide
13	$^{KK}pL_4A_{18}$	Acetyl-KKLAAAAAAAAALWLAAAAAAAAALK2-amide
14	$^{KK}pA_{22}$	Acetyl-KKAAAAAAAAAAAWAAAAAAAAAAAK2-amide

Table 2

Q-ratio and λmax values for peptides with medium-to-long hydrophobic segments. Qratio is defined in Materials and Methods. nd = not determined. Q-ratio and λmax values shown are the average from three samples. Standard deviation is shown for the Q-ratio. The λmax values for individual samples generally differed from the average by no more than ±1 nm.

peptide	DOPC		DOPS		DOPG		POPC/40%chol	
	Q-ratio	λmax	Q-ratio	λmax	Q-ratio	λmax	Q-ratio	λmax
$^{KK}pA_{18}$	36.7±3	358	0.387±0.09	327	nd	nd	nd	nd
$^{RR}pA_{18}$	5.63± 1.6	356	0.135±0.03	327	nd	nd	nd	nd
$^{KK}pL_2A_{18}$	10± 1	357	0.143±0.09	327	nd	nd	nd	nd
$^{KK}pA_{22}$	36.9± 5	360	0.785±0.17	334	nd	nd	nd	nd
$^{KK}pL_4A_{18}$	0.933±.25	335	0.254±0.07	325	0.718±0.16	332	1.94±0.91	349

Table 3

Helix content of membrane-associated peptides in different lipids as determined by circular dichroism. Samples contained 5 or 10 μM peptide in vesicles composed of 500 μM lipid. The remainder of the secondary structure was largely unordered.

Peptide	Lipid	Peptide:Lipid Ratio (mol:mol)	pH	% Helix Content
$^{KK}pL_7A_8$(D10)	DOPC	1:50	4	65
	DOPC	1.50	9	68
	POPC/40%Chol	1:50	4	58
	POPC/POPE	1:50	4	67
	DOPG	1.50	4	68
	DOPG	1:50	5.5	69
	DOPS	1:50	5.5	90
$^{KK}pL_{13}A_2$(D10)	DOPC	1.50	4	71
	DOPC	1:50	9	74
	POPC/40%Chol	1:50	4	66
	POPC/POPE	1.50	4	68
	DOPG	1:50	4	70
	DOPS	1:50	5.5	85
	DOPC	1:100	4	68
	DOPS	1:100	5.5	80
$^{KK}pL_9A_6$(D10)	DOPC	1:50	4	73
	DOPC	1.50	9	74
	DOPS	1:50	5.5	89
	DOPC	1:100	4	70
	DOPS	1:100	5.5	94
$^{KK}pL_{11}A_4$(D10)	DOPC	1:50	4	78
	DOPC	1:50	9	72
$^{KK}pL_4A_{18}$	DOPC	1:50	4	60
	POPC/40%Chol	1:50	4	61
	DOPG	1:50	4	67
	DOPS	1:50	5.5	83
	DOPC	1:100	4	63
	DOPS	1:100	4	86
$^{KK}pA_{18}$	DOPC	1:50	4	71
	DOPS	1.50	5.5	79
$^{KK}pA_{22}$	DOPC	1:50	4	65
	DOPS	1:50	5.5	85
$^{KKKK}pL_{11}A_4$(D10)	DOPC	1.50	4	67
	DOPG	1:50	4	65
^{HH}L12	DOPC	1:50	5.5	76
	DOPS	1:50	5.5	90
	DOPC	1:100	5.5	80
	DOPS	1:100	5.5	90